JOURNAL OF RESEARCH of the National Bureau of Standards—A. Physics and Chemistry
Vol. 78A, No. 3, May–June 1974

Heat Capacities of Polyethylene from 2 to 360 K. II. Two High Density Linear Polyethylene Samples and Thermodynamic Properties of Crystalline Linear Polyethylene

S. S. Chang

Institute for Materials Research, National Bureau of Standards, Washington, D.C. 20234

(February 13, 1974)

Heat capacities of two high density linear polyethylene samples were measured from 2 to 360 K. By incorporating the results from the previous work of this series, thermodynamic properties of completely crystalline linear polyethylene may be estimated. C_p, $H - H_0$, S and $-(G - H_0)$ at 298.15 K for crystalline linear polyethylene are estimated to be 22.60 J K^{-1} mol^{-1}, 3544 J mol^{-1}, 23.02 J K^{-1} mol^{-1} and 3319 J mol^{-1}, respectively. Spontaneous adiabatic temperature drifts were observed in both samples near 240 K. These drifts may be attributed to the enthalpy relaxation phenomena occurring in the glass transformation region.

Key words: Amorphous polyethylene; calorimetry; crystalline polyethylene; extended chain crystals; glass transition temperature; heat capacity; linear polyethylene; polyethylene; thermodynamic properties.

1. Introduction

The heat capacity behaviors of two high density linear polyethylene samples were studied. These two samples were prepared from the same stock from which the standard reference material SRM 1475 for linear polyethylene whole polymer was established. By crystallizing slowly from the melt in vacuum, the degree of crystallinity of the sample was increased from the original value of 71 to 88 percent, as estimated from their densities. Another sample was crystallized under 5000 atm of pressure. The pressure-crystallized sample was composed mainly of extended-chain crystals and has a degree of crystallinity of 96 percent.

By combining the results from this work and from the previous work [1][1] on a sample of SRM 1475 in the condition as received, the thermodynamic properties of 100 percent crystalline linear polyethylene may be estimated.

Large spontaneous temperature drifts were observed in the temperature range centering around 235 – 240 K for both samples when quenched or annealed, as well as for the original sample of SRM 1475 after similar quenching and annealing procedures. These drifts, phenomenologically similar to that observed to occur in the glass transformation range of completely amorphous substances, are the basis of the assignment of the glass transition temperature in polyethylene.

2. Experimental Detail

2.1. Calorimetry

Heat capacity measurements on the two high density linear polyethylene samples were made with the same vacuum adiabatic calorimeter [2] as that used previously for the two samples of standard reference materials, SRM 1475 and SRM 1476 (linear and branched polyethylene whole polymers) in the conditions as received [1].

2.2. Samples

a. Slow Melt-Crystallized Linear Polyethylene

The density and the crystallinity of a sample of SRM 1475 linear polyethylene were increased by melting and recrystallizing the sample slowly in a mold in a vacuum oven. The sample was melted by heating to 170 °C and keeping it there for about 1 hr. It was then cooled to 150 °C in 1 hr. A rate of cooling of 0.75 K h^{-1} was maintained during the period when the sample was cooled from 150 to 90 °C. The sample was then cooled to room temperature at a rate of a few degrees per hour.

The finished sample from the mold was in the shape of a cylinder, 5-cm O.D. and 6.3-cm long, with a hole of 1.3-cm diam in the center. The density of the sample was 0.981 g cm^{-3} at 23 °C as determined in an ethanol-water density gradient column.

Small angle x-ray diffraction patterns were obtained from this sample. The long spacing of the sample

---

[1] Figures in brackets indicate the literature references at the end of this paper.

was increased to 24.7 nm by the slow melt crystallization process. The new value is about twice the original value, 12.1 nm. for the sample of SRM 1475 in the condition as received. The mass of the calorimetric sample was 93.105 g in vacuo. The density values of 0.981 and 0.00117 g cm^{-3} for the sample and for air, respectively, were used to estimate the buoyancy correction. No variation in the densities of the sample, before and after the calorimetric measurement, was detected beyond a range of 0.0005 g cm^{-3}. Helium gas at a pressure of 12.5 cm of Hg was sealed in to facilitate the thermal conduction within the sample container.

b. Pressure Crystallized Linear Polyethylene

The crystallization of linear polyethylene sample under high pressure [3] was carried out as follows. A sample of SRM 1475 linear polyethylene was placed in a steel pressure vessel, 2.5-cm I.D. and 2.5-cm wall thickness, and then pumped down to a pressure of about 1×10^{-4} mm of Hg. After 2 h, a sealing plug was forced into the bore and the vessel was disconnected from the vacuum line. A piston was used to push the plug in until the load reached 5000 lb. The whole vessel was then heated to 210 °C while the position of the piston was kept constant. To do this the load on the piston was increased to about 60,000 lb (equivalent to a pressure of 5150 atm). The piston load was reduced in order to melt the polymer and then increased in 2500 lb increments, followed by 5-min waiting periods, to crystallize the sample under high pressure. Inward creep of the piston during the waiting period, indicative of crystallization, became significant at 48,000 lb load but no apparently isobaric change in piston position occurred. The lack of such a change probably indicates that the pressure is not hydrostatic. At the same piston position, the load was 8000 lb less when being withdrawn then being advanced. If the force at the polymer-sealing plug interface is the average of these, the pressure was 4800 atm when the load applied to the advancing piston was 60,000 lb. After 20 min the heaters were switched off and the load on the advancing piston was kept between 60,000 and 65,000 lb as the vessel was cooled to 100 °C. After cooling to 25 °C over a 15 h period the load was 45,000 lb. The sealing plug was withdrawn and the sample removed.

In order to check the possibility that the increase in the density of the sample is not due to the oxidation of the polymer at elevated temperatures, the sample was subjected to infrared spectroscopic investigations. A film of 0.1 mm thick was prepared from the pressure-crystallized sample according to ASTM Method D–2238–64T. The IR spectrum of this film was examined in the region of 1700–1750 cm^{-1}. The recorded trace indicated only a smooth base line within 0.002 in the absorbancy scale in that region. When the IR spectrum of a film of 0.5 percent CO-ethylene copolymer, 0.04 mm thick and similarly prepared, was examined under the same operational conditions, the absorption peaks in the region 1700–1750 cm^{-1} reached nearly full-scale of the recorder at about 1.23 in absorbancy scale. The peaks of a 0.05 mm film made from 1 percent CO-ethylene copolymer went off-scale in the same frequency region. Hence the oxygen content of the pressure-crystallized sample is probably much less than 10 ppm and no significant oxidation has occurred during the high pressure and high temperature treatments in preparing the sample and the film.

The intrinsic viscosity of the pressure-crystallized sample in 1-chloronaphthalene at 130 °C is 0.915 dl/g. The intrinsic viscosity of the SRM 1475 is 0.890 dl/g as reported in the certificate. Gel-permeation chromatograph, GPC, was also taken for the pressure-crystallized sample in order to detect any changes in the molecular weight distribution. The result of a single GPC run on the pressure-crystallized sample indicates an 8 percent increase in the M_n, a 3 percent increase in the M_w and a 15 percent decrease in the M_z over that of a calibration run of the SRM 1475. Except for the M_z, the changes are within the estimated standard deviations of the molecular weight determinations by GPC for SRM 1475 [4]. Apparently no drastic change of the polymer had occurred during the preparation of the sample under high pressure and high temperature.

The mass of the calorimetric sample was 63.836 g corrected to vacuum. The density values of 0.993 and 0.00117 g cm^{-3} for the sample and for air, respectively, were used to estimate the buoyancy correction. Helium gas at a pressure of 85 mm of Hg at room temperature was sealed in the sample container to facilitate the thermal conduction. The molar mass refers to the mass of the repeating unit $-CH_2-$, 14.027 g.

c. DSC Observations

The melting behavior of the pressure-crystallized linear polyethylene sample was observed in a commercial dynamic differential scanning calorimeter (DSC). The extended-chain crystals of the pressure-crystallized sample melt at a higher temperature than the folded-chain crystals in either the as-received SRM 1475 or the slow melt-crystallized sample. However, just below the main melting peak, there is a small peak or shoulder which occurs at a temperature corresponding to the melting peak of the folded-chain crystals. The ratio of the energies involved for the first (lower temperatures) peak to the main peak varies varies between 2 to 10 percent from sample to sample, indicating some inhomogeneous distribution of small amount of folded-chain crystal in the pressure crystallized sample. Similar behavior in the pressure-crystallized linear polyethylene samples has also been observed by other investigators using differential thermal analysis [3, 5] and DSC [6] techniques. Once the pressure-crystallized sample was melted and then recrystallized at atmospheric pressure, it behaved just like the ordinary linear polyethylene sample.

The energy required to melt the three linear polyethylene samples (as received, slow melt-crystallized, and pressure-crystallized) appears to be a linear function of the degree of crystallinity which is assumed to have a linear relationship with the specific volume of the sample. The heat of fusion for completely crystalline polyethylene is estimated at about 4100 J mol^{-1} from the DSC experiment, if the value of 1.00

cm^3g^{-1} is adopted as the specific volume for 100 percent crystalline polyethylene.

3. Results

3.1. Representation of Data

The results of the heat capacity measurement are tabulated in Table 1 and shown graphically in figure 1. Also shown in figure 1 are the results from the previous work [1] for the linear polyethylene sample SRM 1475 in the condition as received and the branched polyethylene sample SRM 1476 in various conditions. Table 1 is arranged in the order of increasing initial temperature of a series of heat capacity determinations. The series are numbered in chronological sequence in order to facilitate the tracing of thermal history of the sample.

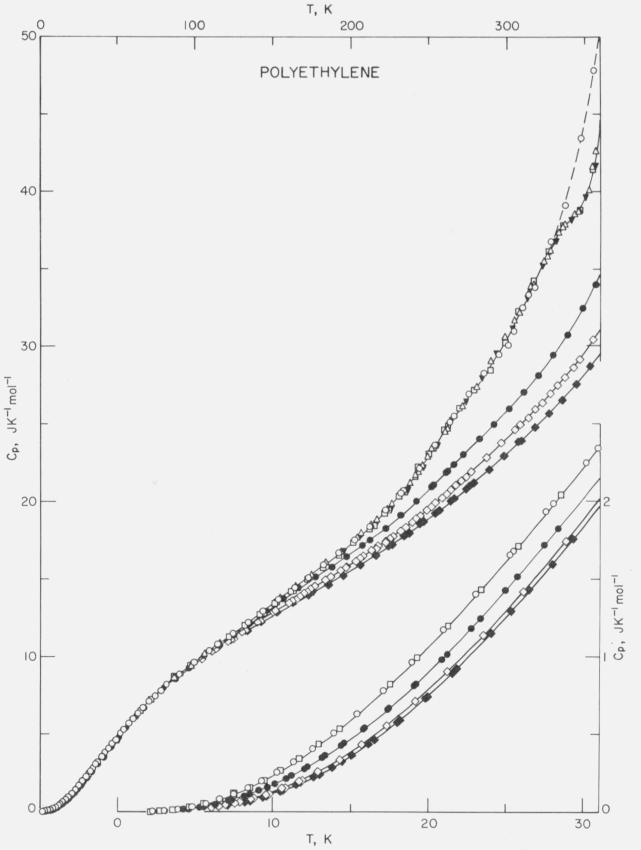

FIGURE 1. *Heat capacities of polyethylene.*

Linear, SRM 1475: ● as received [1], ◇ slow melt-crystallized, ◆ pressure-crystallized. Branched, SRM 1476 [1]: ○ as received, △ stabilized at 360 K and then quenched, □ annealed at 230 K, ▼ slow-cooled.

Quenched samples are produced in the cryostat at a fast cooling rate of 4–5 K/min. Annealed samples are either produced by a slow cooling rate of 1–2 K/h, or by holding at 220 to 225 K for one to three days followed by slow cooling. Series I of both samples represent measurements before any refrigerant being introduced into the cryostat. For the slow melt-crystallized sample, Series II–VI and XI represent heat capacity determinations after a quenching procedure, with the rest of the series represent that following an annealing procedure. For the pressured crystallized sample, Series II and VII–IX represent the measurement on the sample after quenching, while Series III and IV–VII represent that after slow cooling and annealing procedures.

The temperature increment for a heat capacity determination may be inferred from the differences in the mean temperatures of the adjacent determination within the series. Curvature corrections have been added to correct for the effect of the finite temperature rise of a determination. The precision of the measurement above 25 K is in the order of 0.05 percent. Below 25 K, the precision gradually changes to 1 percent at 5 K and about 5 percent at 2 K. The accuracy over most of the temperature range of the measurement is believed to be comparable to the precision as seen from the result of the heat capacity measurement on a Calorimetry Conference standard sample of sapphire [2].

Smoothed heat capacity values at rounded temperatures along with values of other derived thermodynamic functions are listed in table 2. H_0 and S_0 refers to the zero point enthalpy and the residual entropy of the individual samples. Since these samples are expected to have undetermined residual entropies at 0 K. Gibbs free energies for these samples are not given in table 2.

3.2. Estimation of C_p of Crystalline Linear Polyethylene

Heat capacities of linear and branched polyethylene samples from several literature sources as well as those from this research are plotted at selected temperatures as a function of specific volume at room temperature in figure 2. Literature values [7–12] included in figure 2 are those where the densities of the samples are given. The degrees of crystallinity of the samples are interpolated linearly between the specific volume of 1.00 cm^3 g^{-1} for the crystalline part and 1.17 cm^{-3} g^{-1} for the amorphous part.

In order to minimize the effects due to the differences in chemical compositions and due to the differences in the laboratory techniques, the heat capacity of 100 percent crystalline linear polyethylene was estimated only from the results obtained in this laboratory for the three linear polyethylene samples which are derived from the same stock as that used to establish the SRM–1475. The heat capacities of these three samples ranging from 71 to 96 percent crystallinity are represented by the filled circles. The temperatures are denoted by the numbers nearby the straight lines. The straight lines are obtained by a least-squares fitting procedure through the data for the three samples. From 30 to 360 K, the maximum deviations of the data points from the generated lines are less than 0.4 percent. Apparently the two-phase additive model is applicable at high crystalline contents. Since the extrapolated range of crystallinity is only 4 percent, it is believed that the heat capacity of 100 percent crystalline linear polyethylene may be estimated to

TABLE 1. *Heat capacity of linear polyethylene*

(base mole [—CH_2—] = 14.027)

Slow melt-crystallized SRM 1475 ($\rho_{23\,^\circ C}$ = 0.981 g cm^{-3})

T	C_p, J K^{-1}mol^{-1}	T	C_p, J K^{-1}mol^{-1}	T	C_p, J K^{-1}mol^{-1}
	SERIES VIII		SERIES VII		SERIES XI
2.29	0.0014	38.49	2.998	196.07	15.78
2.96	.0034	42.13	3.485	204.96	16.36
3.72	.0070	46.12	4.016	212.83	16.88
4.55	.0132	50.62	4.607	221.64	17.48
5.49	.0234	55.96	5.282	231.38	18.15
6.51	.0385		SERIES XII	241.13	18.87
7.56	.0593	84.99	8.319	250.98	19.64
8.56	.0844	94.24	9.091	260.81	20.48
9.52	.115	104.10	9.839	270.52	21.33
10.51	.151	113.77	10.516		SERIES X
11.60	.198	123.47	11.156	205.49	16.33
12.82	.260		SERIES II	215.02	16.96
	SERIES IX	86.10	8.347	224.57	17.61
6.03	.0304	94.53	9.117	234.13	18.32
6.91	.0457	104.02	9.837	243.78	19.10
7.82	.0654		SERIES III	253.50	19.89
8.75	.0901	110.67	10.31	263.30	20.73
9.67	.120	120.20	10.95	273.08	21.58
10.62	.156	129.91	11.58		SERIES XIV
11.68	.202	139.85	12.22	221.53	17.40
12.88	.263	149.80	12.85	231.27	18.11
14.21	.339	159.70	13.48	241.00	18.87
15.61	.434	169.57	14.10	250.71	19.65
17.21	.553		SERIES XIII	260.41	20.47
19.09	.711	122.61	11.11	270.19	21.33
21.17	.903	131.47	11.69		SERIES V
23.47	1.138	141.44	12.31	238.47	18.68
26.02	1.421	151.55	12.96	248.09	19.44
28.81	1.748	161.60	13.59	258.08	20.25
31.90	2.133	171.51	14.20		SERIES VI
35.32	2.579		SERIES XV	266.89	21.03
39.10	3.081	164.06	13.66	276.47	21.93
45.55	3.940	173.61	14.32	286.14	22.82
52.17	4.806	183.16	14.92	295.87	23.75
57.23	5.438	192.82	15.52	305.58	24.67
63.02	6.118	202.70	16.15		SERIES I
69.24	6.799		SERIES IV	304.88	24.59
76.40	7.523	166.34	13.89	313.62	25.47
84.18	8.246	176.19	14.52	322.76	26.39
		186.23	15.15	332.43	27.42
		196.47	15.81	342.43	28.66
		206.71	16.48		SERIES XVI
		216.75	17.14	308.36	24.92
		226.53	17.81	318.13	25.92
				327.79	26.91
				337.17	27.98
				346.27	29.13
				355.08	30.43

TABLE 1. *Heat capacity of linear polyethylene*—Continued

Pressure-crystallized SRM 1475 ($\rho_{23\,°C}$ = 0.993 g cm^{-3})					
T	C_p, J K^{-1}mol^{-1}	T	C_p, J K^{-1}mol^{-1}	T	C_p, J K^{-1}mol^{-1}
	SERIES VIII		SERIES IV		SERIES III
2.74	.0034	2.32	0.0019	175.30	14.13
3.62	.0061	3.00	.0038	184.83	14.69
4.61	.0126	3.92	.0080	194.77	15.28
5.54	.0210	4.97	.0152	205.11	15.91
6.51	.0335	6.01	.0262	215.51	16.56
7.51	.0513	7.00	.0413	225.65	17.24
8.55	.0744	8.14	.0636		SERIES II
9.58	.1040	9.33	.0956	203.73	15.86
10.63	.1399	10.41	.1310	213.51	16.47
11.74	.1855	11.47	.1718	223.48	17.11
12.96	.2456	12.55	.2250	233.53	17.80
14.38	.3243	13.70	.2841	243.53	18.52
16.06	.4364	15.00	.3625	253.49	19.25
17.90	.5761	16.45	.4638	263.41	20.04
19.77	.7375	18.08	.5903	273.28	20.82
21.75	.9240	19.85	.7424		SERIES VII
23.95	1.152	21.45	.8933	206.68	16.02
26.46	1.433	23.11	1.061	216.39	16.63
29.26	1.763	25.24	1.292	226.32	17.28
32.27	2.144	27.94	1.604	236.31	17.98
35.46	2.562	31.06	1.987	246.22	18.73
38.98	3.032	34.28	2.414	255.99	19.46
43.04	3.576	37.84	2.873	265.62	20.23
47.54	4.178	41.92	3.425	275.31	21.03
52.42	4.818	46.44	4.030		SERIES IX
		51.32	4.674	278.29	21.22
		56.71	5.356	287.99	22.08
			SERIES V	297.74	22.96
		60.51	5.814	307.63	23.85
		66.55	6.497		SERIES I
		73.07	7.185	309.03	23.90
		80.32	7.887	318.10	24.79
		88.58	8.619	326.96	25.64
		97.74	9.352	335.80	26.58
		107.60	10.07	344.60	27.59
		117.99	10.77	353.35	28.71
		128.28	11.41		
			SERIES VI		
		133.00	11.70		
		142.79	12.28		
		152.70	12.86		
		162.63	13.43		
		172.50	13.99		

within 1–2 percent over the majority of the temperature range investigated.

The extrapolated heat capacity values for 100 percent crystalline polyethylene are listed in table 3 along with calculated thermodynamic functions. Also listed in table 3 are linearly extrapolated heat capacity values for amorphous linear polyethylene. The reliability of such an extrapolation for the amorphous phase, especially at temperatures above 250 K, is less certain than that for its crystalline counterpart, not only because the range of extrapolation is much longer than that of the measurement, but also due to the uncertainty in applying the simple two phase additive model over a long extrapolation region. The heat capacity curves for the three linear samples, figure 1, show curvatures concaved upward at temperatures above 300 K. These features are probably caused by premelting or melting of small crystallites. Gibbs free energy functions for the amorphous phase are not included in table 3 because of the existence of an undetermined residual entropy.

The extrapolated heat capacity for crystalline linear polyethylene is a relatively smooth function of temperature. The smoothness may be visualized in the C_p/T, dC_p/dT and $d \ln C_p/dT$ versus T plots, as shown in figure 3. Similar functions for SRM 1475 and SRM 1476 in the condition as received [1] are also shown in figure 3 for comparison. The slight irregularities observed around 290 K in the extrapolated crystalline heat capacity are probably the result of some experimental uncertainties. However, pronounced features centering around 150 and 250 K show up in the behavior of the linear and branched polyethylene samples.

TABLE 2. *Thermodynamic functions of polyethylene*

(units in J, K and mol; base mole [$-CH_2-$] = 14.027)

	Slow melt-crystallized SRM 1475			Pressure-crystallized SRM 1475		
T	C_p	$H-H_0^s$	$S-S_0^s$	C_p	$H-H_0^p$	$S-S_0^p$
5	0.018	0.021	0.006	0.015	0.020	0.005
10	.131	.339	.045	.117	.298	.040
15	.391	1.583	.143	.363	1.434	.129
20	.793	4.490	.307	.757	4.177	.284
25	1.305	9.696	.537	1.265	9.191	.506
30	1.895	17.67	.826	1.854	16.96	.787
35	2.536	28.73	1.166	2.499	27.83	1.121
40	3.202	43.07	1.548	3.168	41.99	1.498
45	3.870	60.75	1.964	3.841	59.52	1.910
50	4.526	81.75	2.406	4.502	80.38	2.349
60	5.766	133.3	3.342	5.750	131.7	3.282
70	6.882	196.7	4.317	6.870	195.0	4.255
80	7.871	270.5	5.301	7.860	268.7	5.238
90	8.747	353.7	6.280	8.736	351.8	6.215
100	9.535	445.2	7.243	9.522	443.1	7.177
110	10.26	544.2	8.186	10.24	542.0	8.119
120	10.94	650.2	9.108	10.90	647.7	9.038
130	11.59	762.8	10.01	11.52	759.8	9.935
140	12.22	881.9	10.89	12.11	878.0	10.81
150	12.86	1007.	11.76	12.70	1002.	11.67
160	13.49	1139.	12.61	13.27	1132.	12.50
170	14.12	1277.	13.44	13.84	1267.	13.33
180	14.74	1421.	14.27	14.42	1409.	14.13
190	15.37	1572.	15.08	15.00	1556.	14.93
200	16.01	1729.	15.89	15.60	1709.	15.71
210	16.66	1892.	16.68	16.22	1868.	16.49
220	17.33	2062.	17.47	16.86	2033.	17.26
230	18.04	2239.	18.26	17.54	2205.	18.02
240	18.79	2423.	19.04	18.26	2384.	18.78
250	19.59	2615.	19.83	19.00	2571.	19.55
260	20.42	2815.	20.61	19.76	2765.	20.31
270	21.31	3023.	21.40	20.56	2966.	21.07
280	22.24	3241.	22.19	21.39	3176.	21.83
290	23.18	3468.	22.99	22.26	3394.	22.59
300	24.14	3705.	23.79	23.14	3621.	23.36
310	25.10	3951.	24.60	24.05	3857.	24.14
320	26.10	4207.	25.41	24.99	4102.	24.92
330	27.16	4473.	26.23	25.97	4357.	25.70
340	28.33	4750.	27.06	27.04	4621.	26.49
350	29.67	5040.	27.90	28.26	4898.	27.29
360	31.23	5345.	28.75	29.72	5188.	28.11
273.15	21.60	3091.	21.65	20.82	3031.	21.31
298.15	23.96	3660.	23.64	22.98	3578.	23.22

The superscripts of s and p for the zero-point enthalpy and entropy values denote the reference states of slow melt-crystallized and pressure-crystallized polyethylene, respectively.

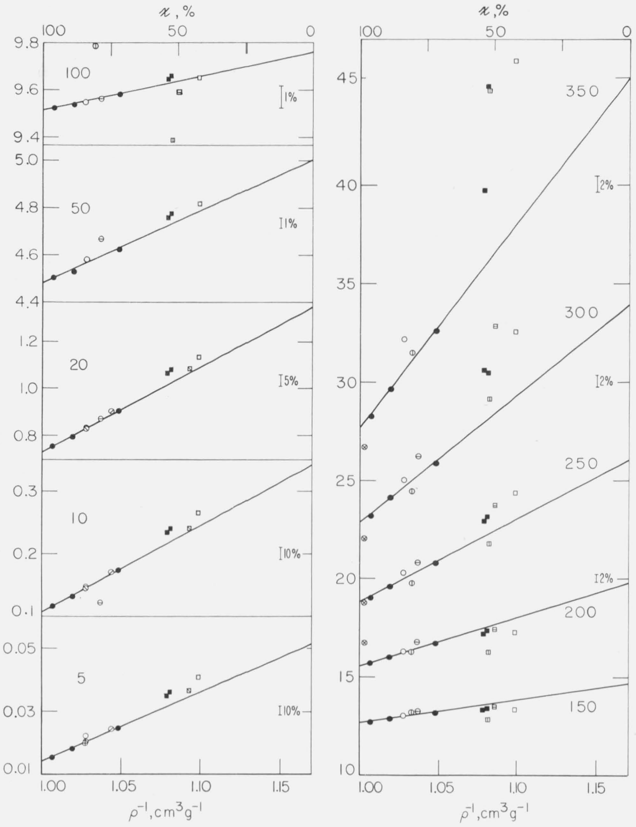

FIGURE 2. *Heat capacity of polyethylene as a function of specific volume.*

Circles—linear polyethylene. Squres—Branched polyethylene. ● ■ This work and previous work [1], ⊖ ⊟ Dainton et al. [7], ○ Isaacs et al. [8], ○□ Passaglia et al. [9], ⊘⊗⧅ Tucker et al. [10], ○ □ Westrum [11], ⊗ Wunderlich [12].

The extrapolated values of crystalline and amorphous linear polyethylene from this investigation are plotted in figure 4 along with estimated values of crystalline, amorphous and liquid polyethylene from other sources. The C_p of ideal CH_2 chain crystal estimated by Broadhurst [13] from the *n*-paraffin data is in general higher than those obtained from this investigation, although the experimental *n*-paraffin values up to 200 K are slightly lower. Between 2 and 30 K, Tucker and Reese's values for the crystalline phase based on their measurements, are very close to ours, and is therefore not shown in figure 4. However, their estimated values from 30 to 150 K, with identical heat capacity for the crystalline and the amorphous phases from 60 to 150 K, lie inbetween our values for the two phases, but closer to our values for the crystalline phase. In an earlier estimate by Wunderlich [14] the values for the crystalline phase is identical to that of the amorphous phase for temperatures below 110 K. These values are somewhat higher than the estimated crystalline heat capacity from this research. At higher temperatures the values for the crystalline heat capacity are also higher than that from this research. The more recent estimate by Wunderlich [15] is based upon Tucker and Reese's estimate up to 150 K and is then made to join at 210 K the results of a differential scanning calorimetric work on extended chain crystals from 180 K [12]. The results of the DSC work are lower than the values for crystalline phase from this research at temperatures above 250 K. In both Wunderlich's estimates, there is a pronounced dip in heat capacity around 250 K. However Wunderlich's calculated values [12] based on a spectrum assigned earlier [16] agree relatively well with the result from this research over a wide temperature range.

For the amorphous phase, the estimation of Tucker and Reese [10] below 30 K agrees relatively well with our estimation for the amorphous phase. Because of the closeness of the two estimations, their values are not shown in figure 4. However their estimation to 150 K and the conclusion that the amorphous and the crystalline phases have identical heat capacity do not agree with the findings from this investigation. Two estimates of heat capacity of amorphous polyethylene have been made by Wunderlich. The earlier one [14] assumes identical heat capacity behavior for the amorphous and crystalline phases for temperatures below 110 K. The more recent one [15] incorporates the estimate by Tucker and Reese for temperatures below 150 K and assumes identical heat capacity values for the two phases between 60 and 210 K. Both Wunderlich's estimates for the amorphous phase are terminated around 250 K by the linear extrapolation of the liquid heat capacity above the melting point.

Heat capacity of the liquid and the supercooled liquid polyethylene from 200 K up has been estimated by many authors. Broadhurst [13] has estimated the C_p of ideal CH_2 chain liquid from *n*-paraffin data from 200 to 370 K. Atkinson, Larkin, and Richardson [17] have based their estimates on their measurement of liquid polyethylene above the melting point and *n*-paraffin data at lower temperatures. Wunderlich's earlier estimates [14] of liquid polyethylene C_p are the linear extrapolations from the liquid heat capacity of a sample of Marlex [2] 50 above the melting point in reference [18]. The more recent estimates [15] of Wunderlich were extrapolated from the average values of a collection of liquid polyethylene data.

3.3. Comparison of Results of Different Polyethylene Samples

Low temperature heat capacity behavior of various polyethylene samples are plotted in figure 5. As mentioned earlier [1], the heat capacities of the linear SRM 1475 sample and the branched SRM 1476 sample in conditions as received agree within 1–2 percent of the values reported for M2 and low density samples, respectively, studied by Tucker and Reese [10]. The reason for the closeness in agreement

---

[2] A commercial material is identified in this paper in order to adequately specify the experimental procedure. Such identification does not imply recommendation or endorsement by the National Bureau of Standards.

TABLE 3. *Thermodynamic properties of extrapolated crystalline and amorphous polyethylene*

(units in J, K, and mol; —CH$_2$—= 14.027)

	Crystalline				Amorphous		
T	C_p	H—H_0^c	S	−(G—H_0^c)	C_p	H—H_0^a	S—S_0^a
5	0.014	0.018	0.005	0.006	0.051	0.057	0.014
10	.106	.267	.036	.092	.341	.943	.126
15	.342	1.323	.118	.451	.800	3.747	.347
20	.727	3.939	.266	1.384	1.346	9.088	.650
25	1.231	8.794	.481	3.225	1.937	17.28	1.014
30	1.819	16.39	.756	6.293	2.547	28.49	1.421
35	2.465	27.08	1.084	10.87	3.167	42.76	1.860
40	3.135	41.07	1.457	17.21	3.788	60.15	2.323
45	3.811	58.44	1.865	25.51	4.398	80.62	2.805
50	4.475	79.16	2.302	35.91	4.991	104.1	3.299
60	5.730	130.3	3.230	63.52	6.115	159.7	4.309
70	6.855	193.3	4.200	100.7	7.144	226.1	5.330
80	7.847	266.9	5.181	147.6	8.079	302.3	6.346
90	8.725	349.9	6.157	204.3	8.934	387.4	7.348
100	9.511	441.1	7.118	270.6	9.737	480.8	8.331
110	10.23	539.9	8.058	346.5	10.53	582.1	9.296
120	10.88	645.4	8.976	431.7	11.35	691.4	10.25
130	11.49	757.3	9.872	526.0	12.27	809.4	11.19
140	12.07	875.1	10.75	629.1	13.38	937.4	12.14
150	12.62	998.6	11.60	740.8	14.60	1077.	13.10
160	13.17	1128.	12.43	861.0	15.78	1229.	14.08
170	13.73	1262.	13.24	989.3	16.88	1393.	15.07
180	14.30	1402.	14.04	1126.	17.89	1567.	16.07
190	14.87	1548.	14.83	1270.	18.81	1750.	17.06
200	15.47	1700.	15.61	1422.	19.72	1943.	18.05
210	16.08	1857.	16.38	1582.	20.66	2145.	19.03
220	16.70	2021.	17.14	1750.	21.70	2356.	20.02
230	17.35	2192.	17.90	1925.	22.91	2579.	21.01
240	18.03	2368.	18.65	2108.	24.32	2815.	22.01
250	18.72	2552.	19.40	2298.	25.95	3066.	23.04
260	19.45	2743.	20.15	2496.	27.64	3334.	24.09
270	20.23	2941.	20.90	2701.	29.29	3619.	25.16
280	21.04	3148.	21.65	2914.	30.86	3920.	26.26
290	21.89	3362.	22.40	3134.	32.36	4236.	27.37
300	22.76	3586.	23.16	3362.	33.85	4567.	28.49
310	23.64	3618.	23.92	3597.	35.45	4913.	29.62
320	24.54	4058.	24.68	3841.	37.26	5277.	30.78
330	25.46	4308.	25.45	4091.	39.43	5660.	31.95
340	26.46	4568.	26.23	4350.	42.09	6067.	33.17
350	27.57	4838.	27.01	4616.	45.33	6503.	34.44
360	28.90	5120.	27.81	4890.	49.21	6975.	35.76
273.15	20.48	3006.	21.14	2768.	29.79	3712.	25.51
298.15	22.60	3544.	23.02	3319.	33.57	4504.	28.28

The superscripts of a and c for the zero-point enthalpy and entropy values denote the reference states of amorphous and crystalline polyethylene respectively.

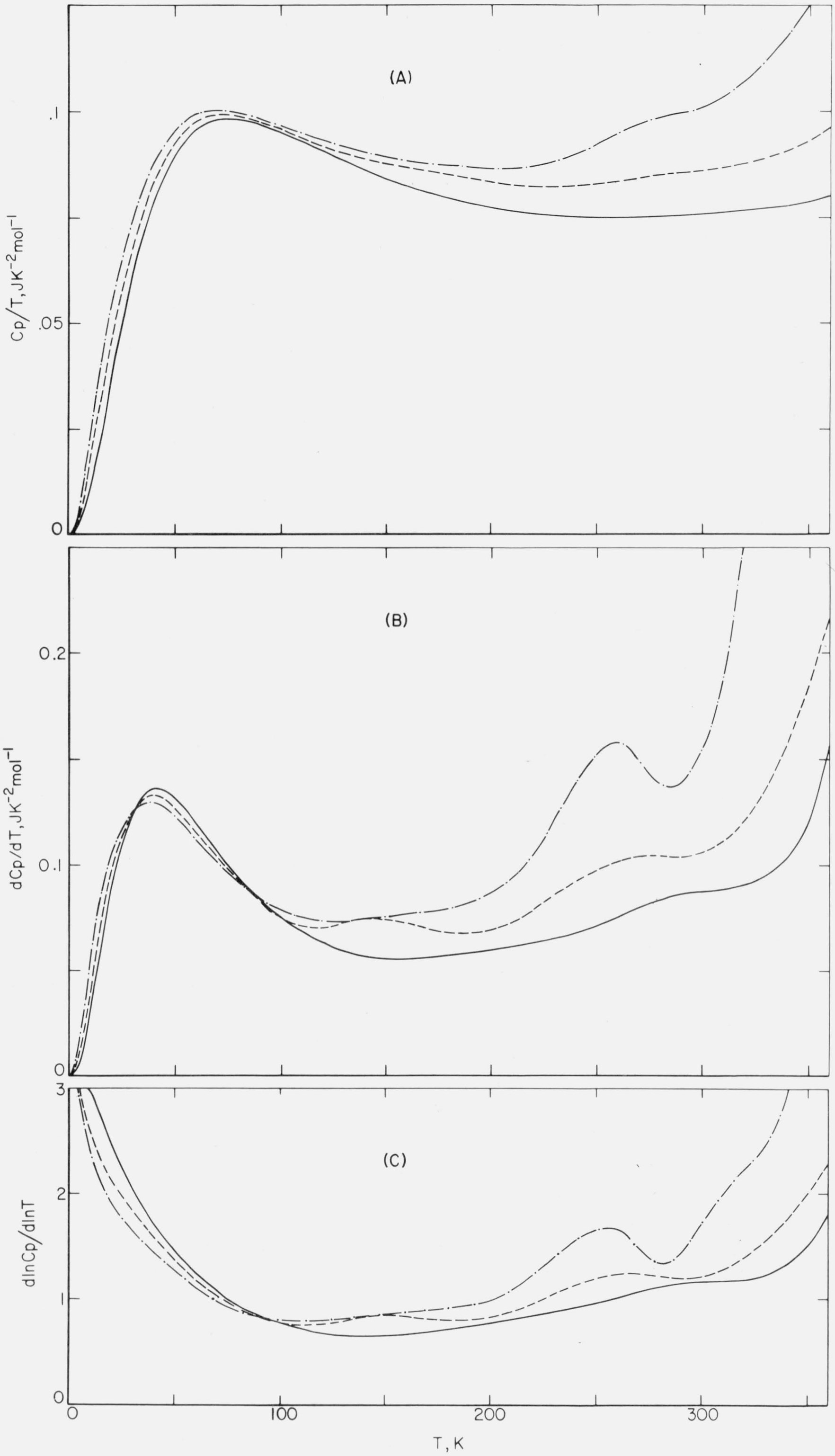

FIGURE 3. (A) C_p/T versus T Plot for Polyethylene.
(B) dC_p/dT versus T Plot for Polyethylene.
(C) $d \ln C_p/dT$ versus T Plot for Polyethylene.
——— estimated crystalline, —— —— linear (SRM 1475 as received), —— · —— branched (SRM 1476 as received)

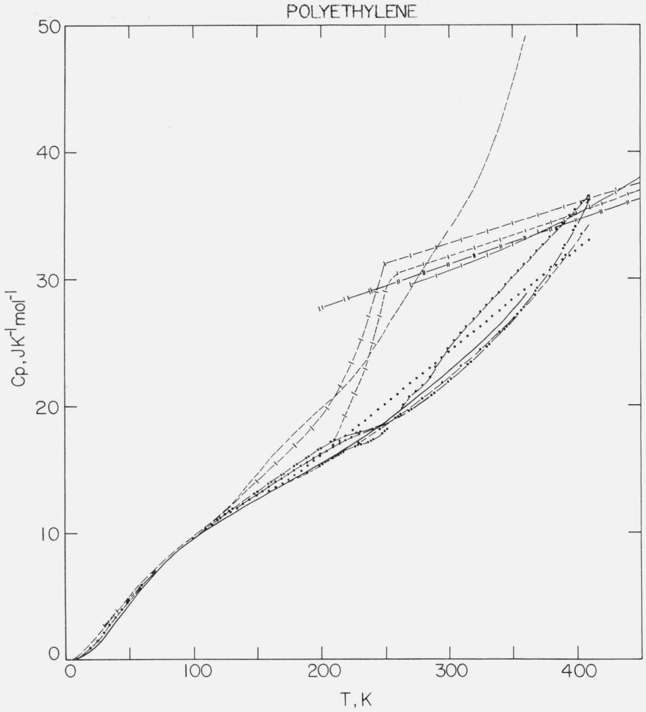

FIGURE 4. *Estimated heat capacity of crystalline and amorphous linear polyethylene.*

Crystalline: This research ———;
Broadhurst [13] · · · · calc., · · · ——— · · · exptl.;
Wunderlich · — · [14], · — — · [12], · · ——— · · [15];
Tucker and Reese [10], not shown.
Amorphous: This research —— ——;
Wunderlich | — — | [14], | — — — | [15];
Tucker and Reese [10], not shown.
Liquid: Broadhurst [13] || — ||;
Wunderlich | — — | [14], | — — — | [15];
Atkinson, Larkin and Richardson [17] | —— |.

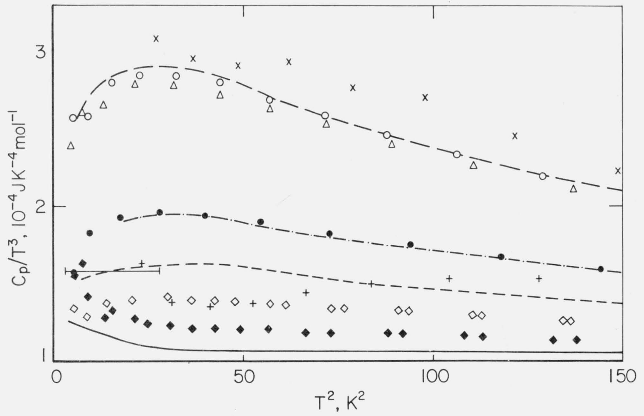

FIGURE 5. *Low temperature heat capacity of polyethylene.*

This work, Linear (SRM 1475): ● as received [1], ◇ slow-melt crystallized, ◆ pressure crystallized, ——— estimated 100 percent crystalline; Branched (SRM 1476) [1]: ○ as received. △ annealed. Isaacs et al. [8]: ——|——|. Tucker et al. [10]: —— —— branched. —— · —— linear (M1), — — — (M2). Westrum [11]: × branched (DYNH), + linear (Marlex 50).

is probably due to their respective similarities in densities. The difference in the densities for the linear polyethylene samples is about 0.004 g cm^{-1} and that for the branched samples is about 0.01 g cm^{-1}.

The linear extrapolation of C_p versus crystallinity below 5 K is probably strongly influenced by the C_p of the pressure-crystallized sample, which shows an upsweep in C_p/T^3 as the temperature is lowered. The reason for this particular behavior to show up only in the sample consisting of mainly extended chain crystals is unknown. If the data of the pressure-crystallized sample below 5 K is not used in the extrapolation, C_p/T^3 for the crystalline phase below 15 K is within 5 percent of a constant 1.05×10^{-4} J K^{-4} mol^{-1}. Tucker and Reese [10] obtained a value of 1.104×10^{-4} J K^{-4} mol^{-1} for C_p/T^3 at 0 K.

A sensitive way of detecting any irregularities in the heat capacity behavior of an individual sample is to remove from the observed heat capacity the contribution from the relatively smooth crystalline heat capacity. The differences in the heat capacity of the three linear polyethylene samples, derived from SRM 1475, from the extrapolated crystalline heat capacity are plotted in figure 6. The short vertical bars at various temperatures indicate the magnitude of 1 percent of extrapolated heat capacity for crystalline linear polyethylene. For the two high density samples, systematic deviations due to the quenching and annealing processes are noticable in the temperature region from 170 to 240 K. The heat capacity of the annealed sample is about 0.1 to 0.2 percent lower than that of the quenched sample. The linear polyethylene sample SRM 1475 in the condition as received [1] has not been subjected to similar annealing and quenching treatments. A hump around 25 K is observed in the heat capacity differences of all three samples. The occurrence and the magnitude of the humps can generally be attributed to the differences in the specific volumes among the different samples [24]. The heat capacity differences of all three samples reach a minimum around 100 K. As shown in figure 2, most of the heat capacity values at 100 K of various linear and branched samples from different laboratories are within a spread of 1 percent.

The heat capacity differences rise sharply after the minimum at 100 K, and level off somewhat around 160 K. This behavior has also been observed by Beatty and Karasz [25] in a sample of high molecular weight linear polyethylene in the temperature region around 130 to 160 K and was considered by them to be the glass transition region for polyethylene. However, the heat capacity differences in figure 6 indicate another region of rapid rise around 230 to 270 K. In this temperature range, Beatty and Karasz have only noted a change of slope in the heat capacity behavior of their sample. Because the changes involved in the heat capacity "irregularities" are in the order of a few percent and spread over a wide temperature range, heat capacity determination alone may not be sufficient to indicate the occurrence of the glass transition in semicrystalline polyethylene.

Heat capacities of linear polyethylene from various literature sources are compared in figure 7 with the extrapolated heat capacity for crystalline linear polyethylene as the base line. The comparisons of branched polyethylene data, including the study of SRM 1476

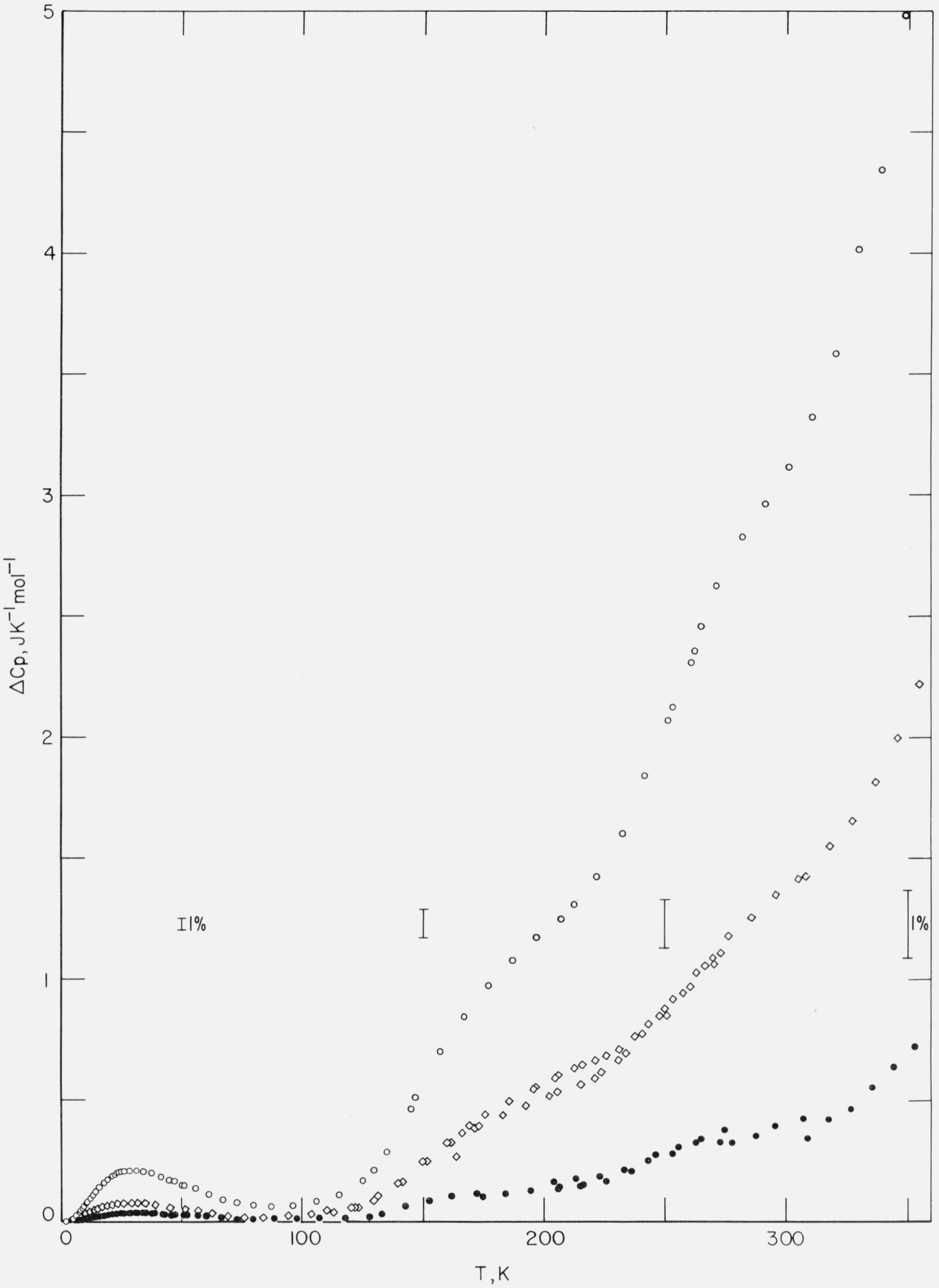

FIGURE 6. *Comparison of heat capacities of linear polyethylene samples versus estimated crystalline heat capacity.*

SRM 1475: ○ as received [1]. ◇, slow crystallized, ● pressure crystallized.

from this laboratory [1] are shown in figure 8. The data are included in the comparison only if they are reported in tabular or analytical form. Data reported in graphical form are not included. When heat capacity values are reported at rounded temperatures, the curves shown in figures 7 and 8 may have been arbitrarily smoothed within the limits of the roundoff error of the reported values.

The results of the comparison shown in figures 7 and 8 are in general self-explanatory. A hump around 25 K in the difference curves, similar to that shown in figure 6, appears in all low temperature measurements. Two regions of more abrupt rise in heat capacity around 150 and 250 K may be noticed in the studies of linear polyethylene samples by Dainton et al. [7], and by Westrum [11], similar to the findings from this

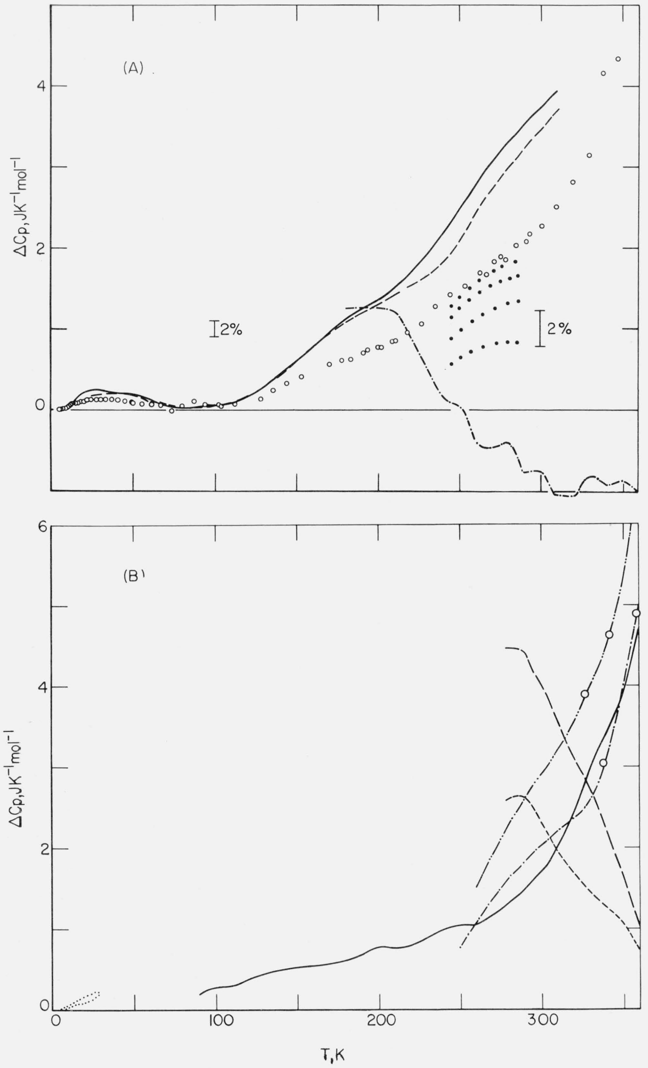

FIGURE 7. *Comparison of literature linear polyethylene heat capacity values.*

Baseline: crystalline linear polyethylene heat capacity from this work.
A. ○ Marlex 50, Westrum [11]; ——— Marlex 50, —— —— Rigidex 50, Dainton et al. [7]; ——·—— Wurderlich [12]; · · · · · single crystals, Richardson [19].
B. —— Linear, Passaglia et al. [9] · · · · M1 and M2, Tucker et al. [10]; —— · —— Annealed, —— · · —— Granular, Dole et al. [13]; —— —— GD, — — — GC, Wilski [14].

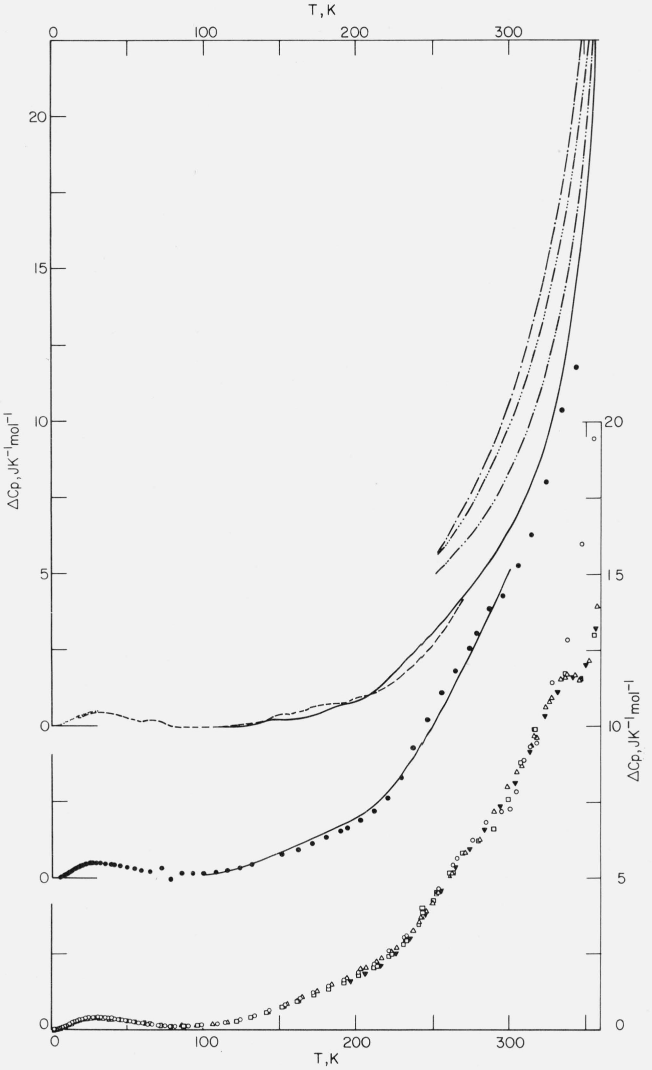

FIGURE 8. *Comparison of branched polyethylene heat capacity values.*

Baseline: crystalline linear polyethylene from this work.
Lower curves: SRM 1476 [1]. same legend as in figure 1.
Middle curves: ● E. F. Westrum [11]; ——— Dainton [7].
Upper curves: · · · Tucker and Reese [10]; — — — Sochava [20, 21]; —— Passaglia and Kevorkian [9]; —— · ——, —— · · ——, —— · · · —— Dole [19].

laboratory [1]. Similar behaviors are noticeable in the measurements on branched samples by Westrum and by this laboratory. The dip around 300 K in Westrum's heat capacity curve for branched polyethylene is probably effected by long storage of the sample near room temperature. Similar features have been noticed in the branched polyethylene sample studied in this laboratory. The irregularities in Westrum's data around 80 to 90 K is presumably due to the temperature scales used. The effect of joining the International Practical Temperature Scale of 1948 and the NBS 1955 Provisional Temperature Scale at 90 K have been noted elsewhere [26, 27].

Sochava's sample [22, 23] is probably a branched polyethylene since its heat capacity behavior follows the pattern of other branched polyethylene samples. The low temperature behavior of this sample is similar to the branched polyethylene studied by Tucker and Reese [10], Westrum [11] and this laboratory [1]. The high temperature behavior of this sample is very similar to that of the branched polyethylene studied by Passaglia and Kevorkian [9]. Passaglia and Kevorkian's result on linear and branched polyethylene indicates that the heat capacity of the higher density linear sample is about 3–4 percent higher than that of the lower density branched sample at temperatures below 180 K. This indication is probably not real. The authors have pointed out in the paper that there have been experimental difficulties, and they have cited an uncertainty of 3–4 percent in the branched polyethylene and about 1 percent in the linear polyethylene measurements.

3.4. Adiabatic Temperature Drift and Glass Transition Temperature

The glass transition temperature of polyethylene has been assigned a value ranging from 130 to 250 K depending on the method of observation and on the investigators. The classical calorimetric and dilatometric methods of observing a break in the enthalpy or volume versus temperature curves, or a discontinuity in the heat capacity or thermal expansion coefficient behaviors, have difficulties in clearly demonstrating the occurrence of the glass transition phenomena in highly crystalline polyethylene. In the more sensitive ΔC_p versus T plot, figure 6, one observes two areas where irregularities occur over a relatively wide temperature range. In both regions the magnitude of the irregularity seems to be proportional to the amorphous content. However, only in the high temperature region, spontaneous thermal relaxation behavior, similar to the behavior of other completely amorphous substances, has been observed for the polyethylene samples. Thus the glass transition of polyethylene is limited to the higher temperature region of the heat capacity irregularities.

The detection of the kinetic nature of the glass transition phenomena in polyethylene by means of the observations of spontaneous adiabatic temperature drift in the glass transition region has been discussed in more detail elsewhere [28]. The following serves as a summary as well as a supplement.

The drift observation is enhanced by quenching and annealing treatments of the sample. In adiabatic calorimetry, the average heating rate during the heat capacity measurement is relatively constant, in the order of 10 K h^{-1}. Quenching is defined as a cooling rate to produce a glass at a much greater rate than the normal rate of observation. The cooling rates for quenching the sample in the calorimeter is generally in the order of 5 K min^{-1}. The annealing of a glass can either be achieved by a very slow rate of cooling in comparison to the rate of observation, or by holding for a couple of days at temperatures somewhat below the glass transition temperature of the quenched glass. A slow cooling rate of less than 1 K h^{-1} can easily be achieved. When a quenched glass is heated to temperatures near the glass transition region, sufficient mobility in the quenched glass allows it to relax toward the configurations of the supercooled liquid. If the sample is kept in an adiabatic environment, this relaxation shows up as a spontaneous temperature rise of the sample. This phenomena can usually be detected from some 50 K below the glass transition temperature, for materials having T_g around 200 to 300 K. Annealed glass can easily be overheated to temperatures above its glass transition temperature before its viscosity decreases to a low enough level to allow significant configurational relaxation to occur. Therefore the over-heated annealed glass relaxes toward the supercooled liquid state by spontaneously lowering its temperature under adiabatic conditions. The spontaneous heating and cooling of the quenched and annealed vitreous sample near the glass transition region have been observed for many vitreous materials as cited in reference [28]. Drifts have also been noted in some recent calorimetric studies on vitreous substances [29, 30]. The drift method has also been applied to the locating of the T_g of partially crystalline poly-1-pentene [31].

The total observed temperature in adiabatic calorimetry may come from three different sources, namely, the thermometer current, the heat transferred between the calorimeter and the shield, and the thermal effects generated by the sample itself. A steady thermometer current of 2 mA flowing through a 25-Ω (0 °C) platinum resistance thermometer produces approximately 0.1 T/273 mW of power. At around 250 K, under strict adiabatic conditions this power dissipation will cause a positive drift of the order of 0.03 mK min^{-1} to appear for the calorimeter loaded with polyethylene. The heat transfer coefficient for the loaded calorimeter at 250 K is about 1 mK min^{-1} per kelvin of temperature difference between the calorimeter and the adiabatic shield. With the short term temperature difference settable and controllable to within 1 mK, the positive drift produced by the thermometer current can be detected. Long term systematic variation in the drift has been observed to occur in the order of 0.05 mK min^{-1} per hour. The drift observable at the same temperature on different days may be different due to the residual emf in the differential thermocouple circuit. The residual emf in the heater and in the thermometer circuits is always less than 1 μV and varies slowly in time and temperature. Assuming a similar order of magnitude of the residual emf in the differential thermocouple circuit, a temperature difference in the order of 20 mK may exist between the adiabatic shield and the sample container. Coupled with the thermal transfer coefficient, a long term variation in the drift in the order of 0.05 mK min^{-1} may be expected.

In the temperature region around 150 K, some irregularity shows up in the ΔC_p plot, figure 6. The magnitude of the irregularity seems to be more pronounced in the linear sample than that in the branched sample, figure 8, it also seems to be proportional to the amorphous content. However no significant and long thermal drift is observed in this temperature region. One might associate this irregularity to the onset of the so-called crankshaft motion or other forms of segmental motion of the polyethylene chain in the amorphous phase. Branching of the chain increases the volume to be swept by this kind of motion and thus may hinder or move the onset to much higher temperature. A more pronounced C_p irregularity has been observed in a high molecular weight linear polyethylene sample [25].

Near 250 K, heat capacity irregularities show up in all three linear polyethylene samples, figure 6. The magnitude of the irregularity seems to be proportional to the amorphous content of the sample. Similar behavior may be seen in branched samples, figure 8. Significant spontaneous warming and cooling of the sample after quenching and annealing, respectively, also show up in this temperature region. The calorimetric temperature drift, observed at 30 min after the termination of each energy input for the three linear polyethylene samples under both quenched and annealed conditions, are shown in figure 9. The drift behavior for the branched polyethylene sample was shown in reference [1]. Although the maximum magnitude of the observed drift is about one order of magnitude smaller than that observed in completely vitreous materials, the observed magnitude is still one order of magnitude greater than the contribution from the thermometer current and from the heat leak in the calorimeteric system. The magnitude of the maximum observed drift seems to be proportional to the amorphous content of the sample. However, the temperature at which the maximum drift occurs does not vary significantly as a function of the crystallinity of the sample. All three quenched samples show spontaneous warming drift peaks at temperatures around 235 K, and the annealed samples indicate cooling peaks near 245 K. Therefore in analogy with the behaviors observed for completely vitreous materials as cited in reference [28] and elsewhere, the glass transition temperature for the linear polyethylene sample may be assigned a value of 240 ± 5 K. This assignment is in good accord with a recent volume relaxation study on polyethylene samples [32]. The drifts for the two densified samples have been observed along with the heat capacity measurements reported in this paper. During the heat capacity measurements for the SRM 1475 in the condition as received [1], no annealing and quenching treatments were applied. Therefore the same sample was reloaded in the calorimeter and the drift behavior was observed following similar annealing and quenching treatments to those for the two high density samples.

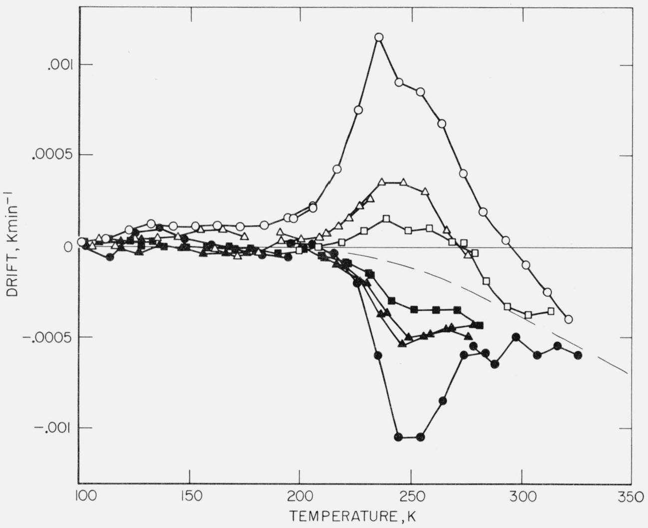

FIGURE 9. *Spontaneous adiabatic temperature drift of linear polyethylene.*

○ ● SRM 1475 as received, △ ▲ slow melt-crystallized, □ ■ pressure crystallized. Open symbols, quenched samples; filled symbols, annealed samples. Dashed line represents drift due to heat exchange alone under similar operational conditions.

The author wishes to thank C. H. Pearson in assisting in the calorimetric measurements and D. W. Brown for the preparation of the pressure-crystallized sample. He also wishes to thank G. T. Davis, Cheng-Hsiung Hsieh,[3] R. G. Christensen and G. Ross for the characterization of the samples by small-angle X-ray diffraction, IR spectroscopy, viscosity and gel-permeation chromatography, respectively.

4. References

[1] Chang, S. S., and Bestul, A. B., J. Res. Nat. Bur. Stand. (U.S.), **77A** (Phys. and Chem.), No. 4, 395–405 (July–Aug. 1973).
[2] Sterrett, K. F., Blackburn, D. H., Bestul, A. B., Chang, S. S., and Horman, J. A., J. Res. Nat. Bur. Stand. (U.S.), **69C** (Eng. and Instr.), No. 1, 19–26 (Jan.–Mar. 1965).
[3] Wunderlich, B., and Arakawa, T., J. Polymer Sci. A–2, 3697 (1964).
[4] Ross, G., and Frolen, L., J. Res. Nat. Bur. Stand. (U.S.), **76A** (Phys. and Chem.), No. 2, 163–170 (Mar.–Apr. 1972).
[5] Kardos, J. L., Baer, E., Geil, P. H., and Koenig, J. L., Kolloid Z. **204,** 1 (1965).
[6] Calvert, P. D., and Uhlmann, D. R., J. Polymer Sci. A–2, **10,** 1811 (1972).
[7] Dainton, F. S., Evans, D. M., Hoare, F. E., and Melia, T. P., Polymer **3,** 277 (1962).
[8] Isaacs, L. L., and Garland, C. W., J. Phys. Chem. Solids **23,** 311 (1962).
[9] Passaglia, E., and Kevorkian, H. K., J. Appl. Polymer Sci. **7,** 119 (1963).
[10] Tucker, J. E., and Reese, W., J. Chem. Phys. **46,** 1388 (1967).
[11] Westrum, E. F., Jr., unpublished.
[12] Wunderlich, B., J. Phys. Chem. **69,** 2078 (1965).
[13] Broadhurst, M. G., J. Res., Nat. Bur. Stand. (U.S.), **67A** (Phys. and Chem.), No. 3, 233–240 (May–June 1963).
[14] Wunderlich, B., J. Chem. Phys. **37,** 1203 (1962).
[15] Wunderlich, B., and Baur, H., Adv. Polymer Sci. **7,** 261 (1970).
[16] Wunderlich, B., J. Chem. Phys. **37,** 1207 (1962).
[17] Atkinson, C. M. L., Larkin, J. A., Richardson, Y. M. J., J. Chem. Therm. **1,** 435 (1969).
[18] Wunderlich, B., and Dole, M., J. Polymer Sci. **24,** 201 (1957).
[19] Richardson, M. J., Trans. Faraday Soc. **61,** 1876 (1965).
[20] Wilski, H., Kunstoffe **50,** 281 (1960).
[21] Dole, M., Hettinger, W. P., Jr., Larson, N. R., and Wethington, J. A., Jr., J. Chem. Phys. **20,** 781 (1952).
[22] Sochava, I. V., Doklady Akad. Nauk SSSR **130,** 126 (1960).
[23] Sochava, I. V., and Trapeznikova, O. N., Soviet Phys. Doklady **2,** 164 (1957).
[24] Guttman, C. M., J. Chem. Phys. **56,** 627 (1972).
[25] Beatty, C. L., and Karasz, F. E., Bull. Am. Phys. Soc. Ser. II, **16,** 1391 (1971).
[26] Furukawa, G. T., and Reilly, M., J. Res. Nat. Bur. Stand. (U.S.), **69A** (Phys. and Chem.), No. 1, 5–12 (Jan.–Feb. 1965).
[27] Roder, H. M., J. Res. Nat. Bur. Stand. (U.S.), **69A** (Phys. and Chem.), No. 6, 527–530 (Nov.–Dec. 1965).
[28] Chang, S. S., J. Polymer Sci. Part C, 43, (1973).
[29] Matsuo, T., Oguni, M., Suga, H., and Seki, S., Proc. Japan Acad. **48,** 237 (1972).
[30] Haida, O., Matsuo, T., Suga, H., and Seki, S., Proc. Japan Acad. **48,** 489 (1972).
[31] Bourdariat, J., Isnard, R., and Odin, J., IUPAC Intl. Sym. Macromol., Aberdeen, September 1973.
[32] Davis, G. T., and Eby, R. K., J. Appl. Phys. **44,** 4274 (1973).

(Paper 78A3–819)

---

[3] Guest Worker at NBS from the Union Industrial Research Institute, Hsing-Chu, Taiwan, Republic of China.